# Supporting Information: Evaluation of Global Teleconnections in CMIP6 Climate Projections using Complex Networks

Clementine Dalelane, Kristina Winderlich, Andreas Walter

June 2, 2022

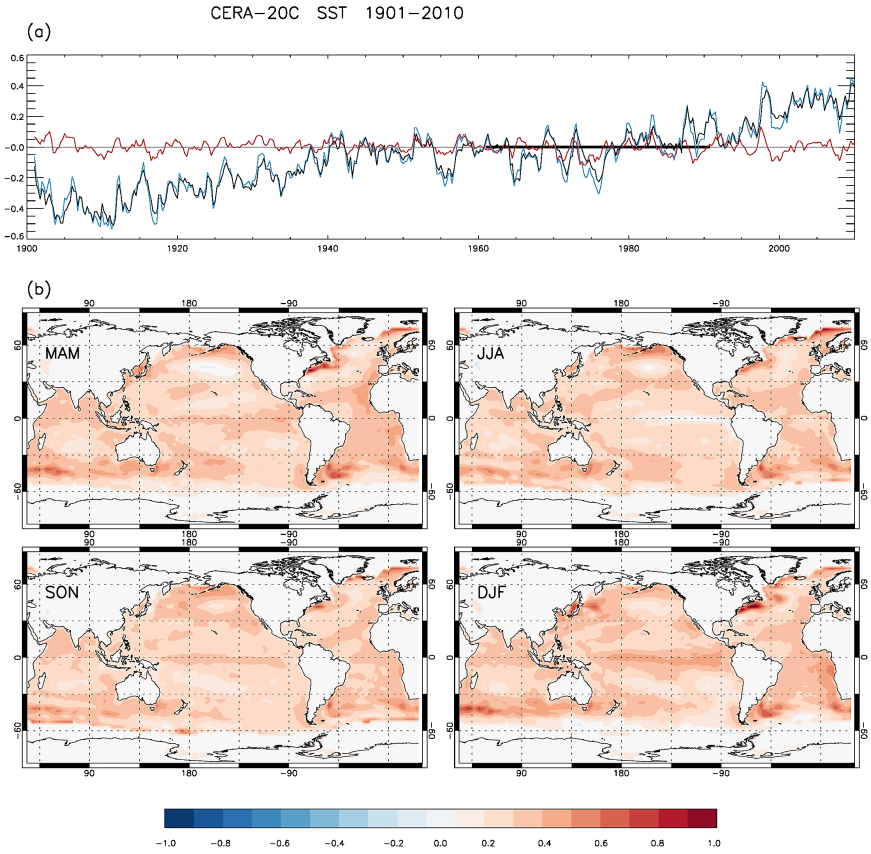


Figure S1: Season-reliant trend-EOF of the CERA-20C SST fields over the time period 1901–2010. (a) Global mean SST anomaly (GMSSTa) wrt. reference period 1961–1990 (black), forced component of GMSSTa (blue), residual (red). (b) Seasonal trend-loading patterns in physical space (arbitrary units normalized to [-1,1] over all seasons).

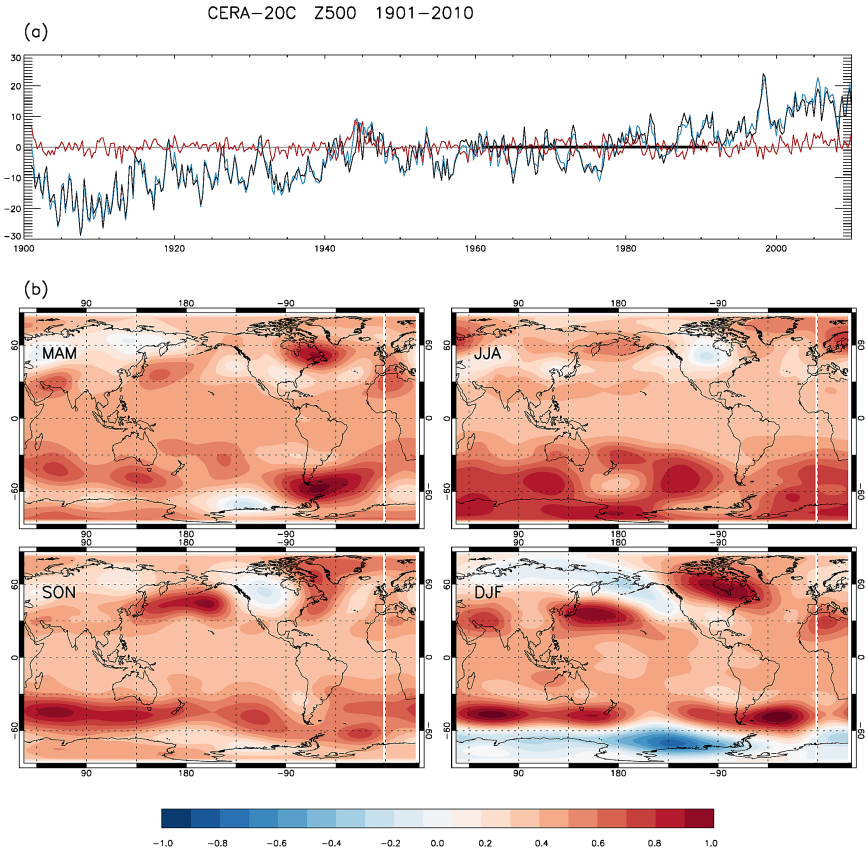


Figure S2: Season-reliant trend-EOF of the CERA-20C Z500 fields over the time period 1901–2010. (a) Global mean Z500 anomaly (GMZ500a) wrt. reference period 1961–1990 (black), forced component of GMZ500a (blue), residual (red). (b) Seasonal trend-loading patterns in physical space (arbitrary units normalized to [-1,1] over all seasons).

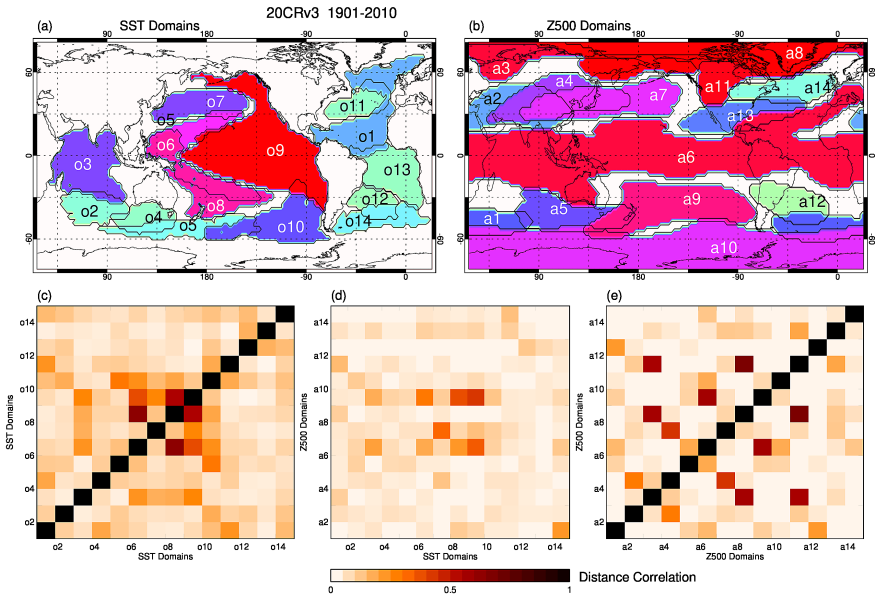


Figure S3: Domains of the 20CRv3 (a) SST and (b) Z500 fields over the time period 1901–2010 (arbitrary colors). Maximum lagged distance correlation links between (c) SST and (e) Z500 domains and (d) cross-links.

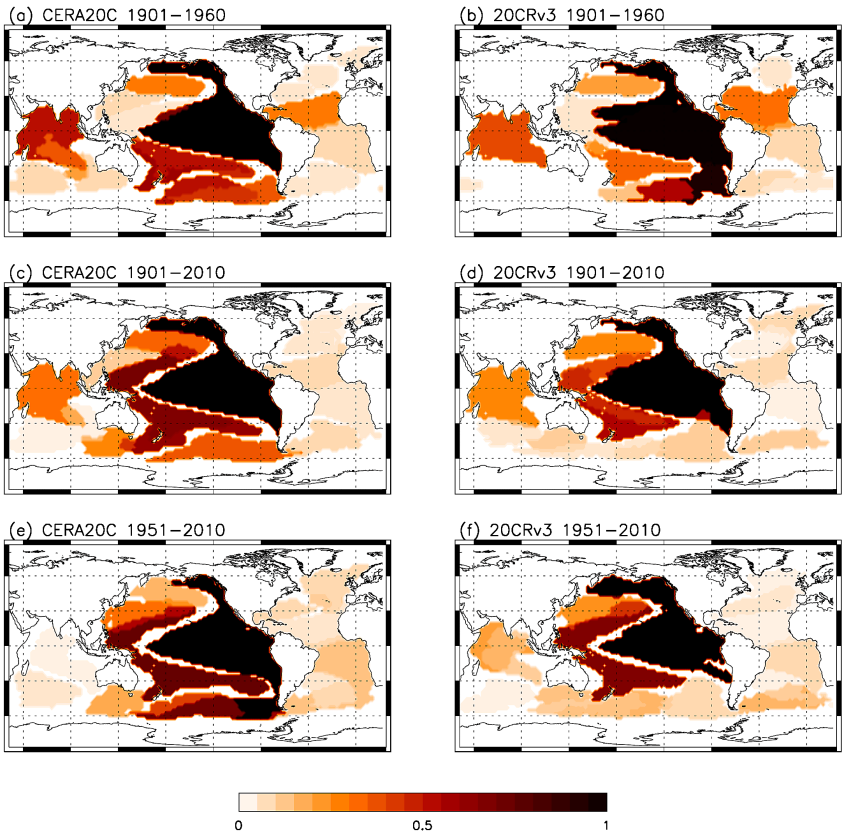


Figure S4: Spatially distributed maximum lagged distance correlation links between the ENSO SST domain (black) and all other SST domains in reanalyses. (a),(c),(e) CERA-20C, (b),(d),(f) 20CRv3, (a),(b) time period 1901–1955, (c),(d) time period 1901–2010, (e),(f) time period 1951–2010.

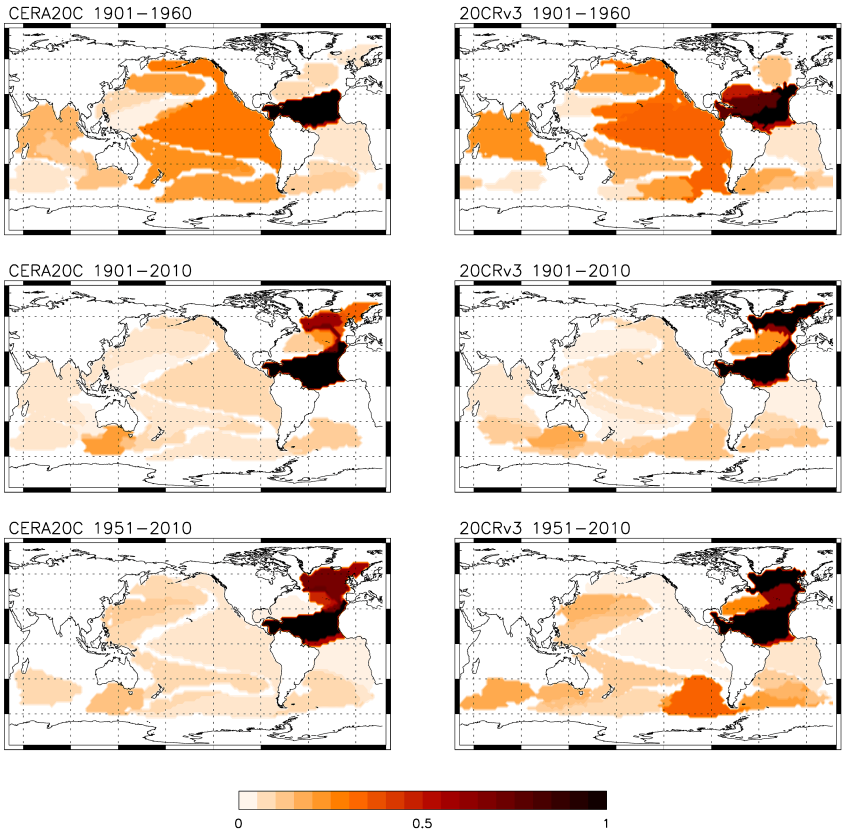


Figure S5: Spatially distributed maximum lagged distance correlation links between the AMO SST domain (black) and all other SST domains in reanalyses. (a),(c),(e) CERA-20C, (b),(d),(f) 20CRv3, (a),(b) time period 1901–1955, (c),(d) time period 1901–2010, (e),(f) time period 1951–2010.

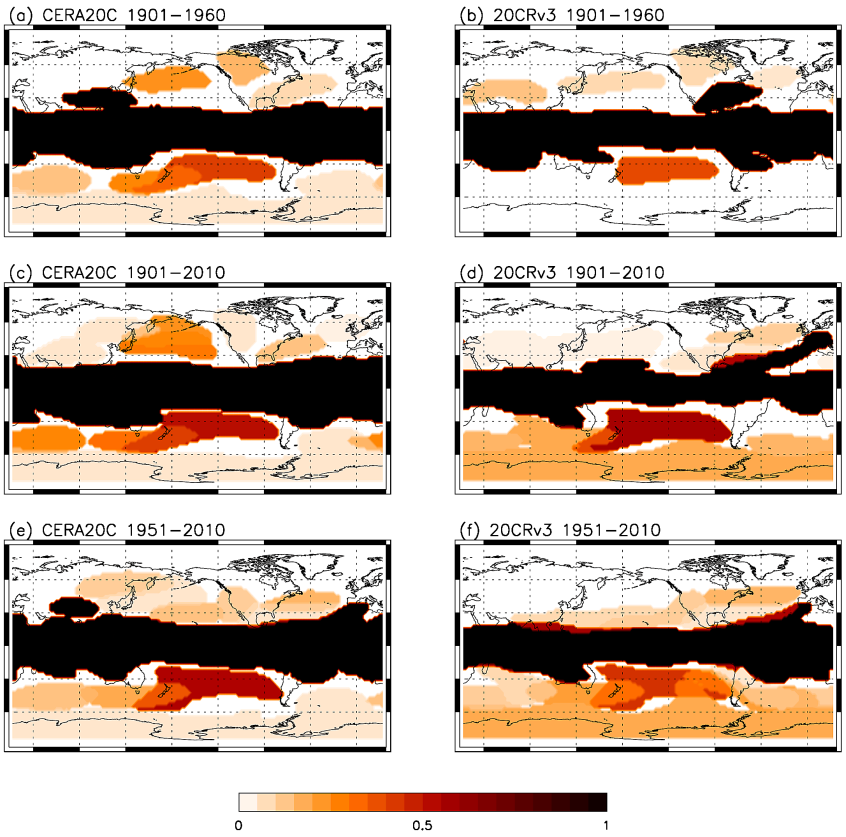


Figure S6: Spatially distributed maximum lagged distance correlation links between the Tropical Belt Z500 domain (black) and all other Z500 domains in reanalyses. (a),(c),(e) CERA-20C, (b),(d),(f) 20CRv3, (a),(b) time period 1901–1955, (c),(d) time period 1901–2010, (e),(f) time period 1951–2010.

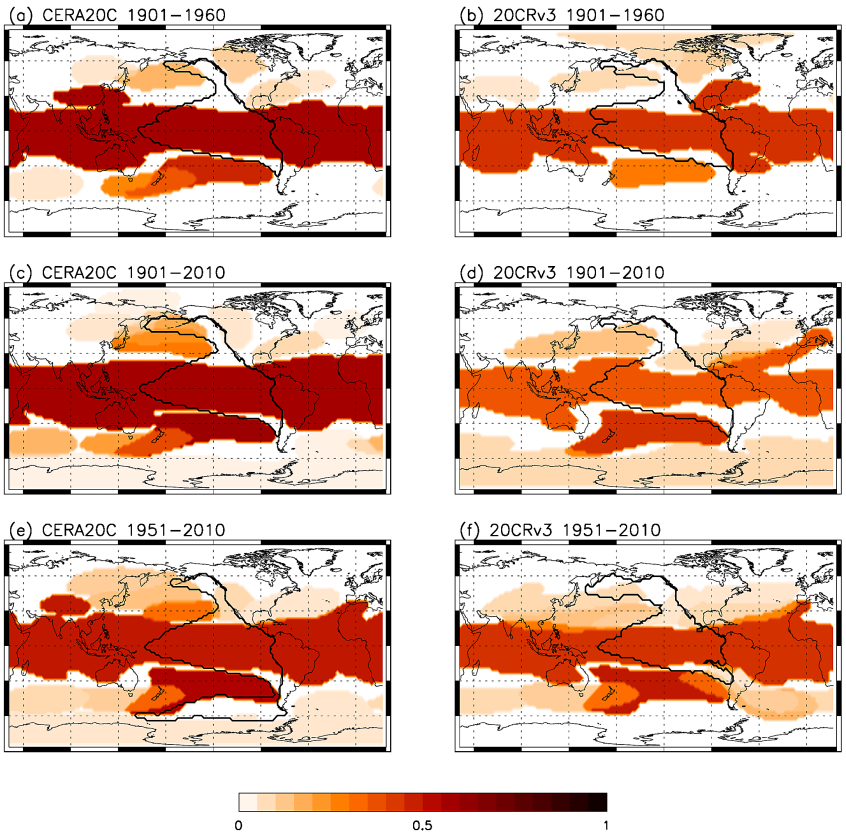


Figure S7: Spatially distributed maximum lagged distance correlation cross-links between the ENSO SST domain (contoured) and all Z500 domains in reanalyses. (a),(c),(e) CERA-20C, (b),(d),(f) 20CRv3, (a),(b) time period 1901–1955, (c),(d) time period 1901–2010, (e),(f) time period 1951–2010.

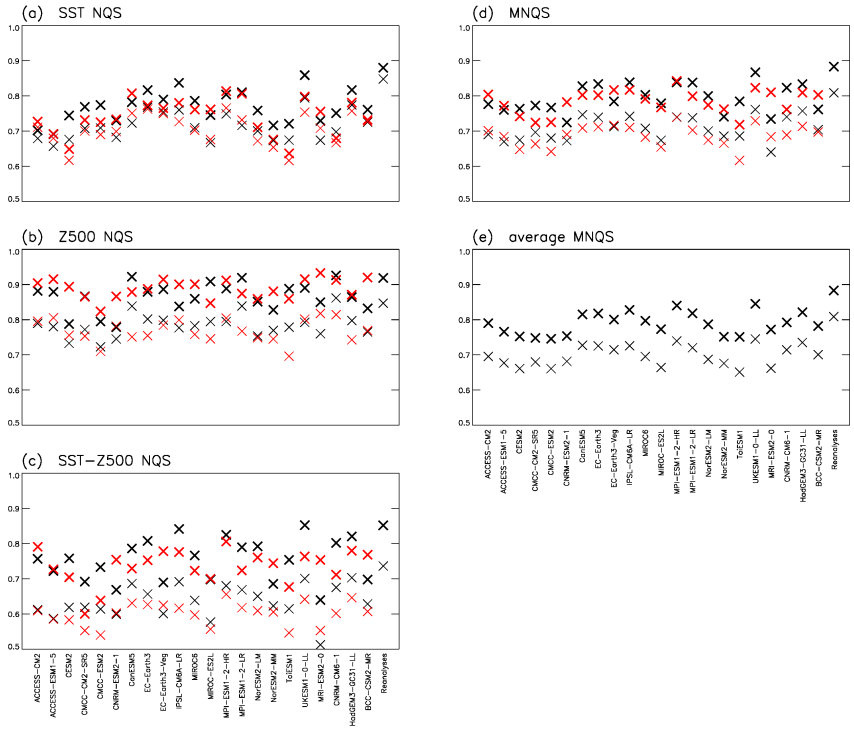


Figure S8: Network Quality Scores (bold) and point-wise Network Quality Scores (thin) of CMIP6 Models wrt. CERA-20C (black) and 20CRv3 (red) over the time period 1951–2010. (a) networks for SST fields, (b) networks for Z500 fields, (c) cross-networks between SST and Z500 fields. (d) Multivariate Networks Quality Scores, (e) average Multivariate Network Quality Score.

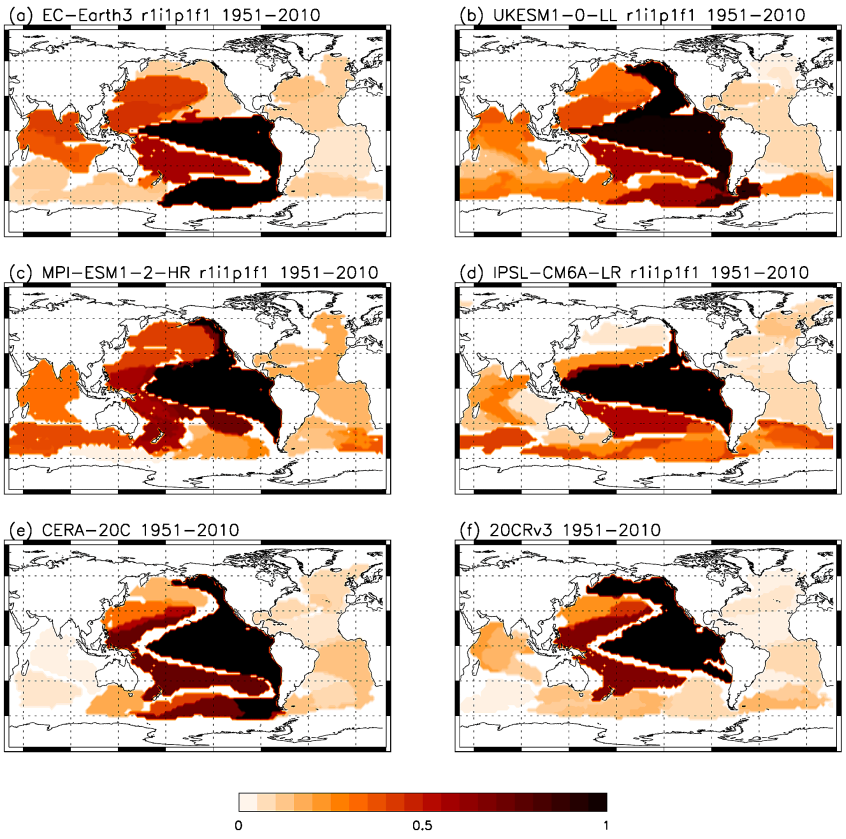


Figure S9: Spatially distributed maximum lagged distance correlation links between the ENSO SST domain (black) and all other SST domains in reanalyses over the time period 1951–2010. (a) EC-Earth3, (b) UKESM1-0-LL, (c) MPI-ESM1-2-HR, (d) IPSL-CM6A-LR,(e) CERA-20C, (f) 20CRv3

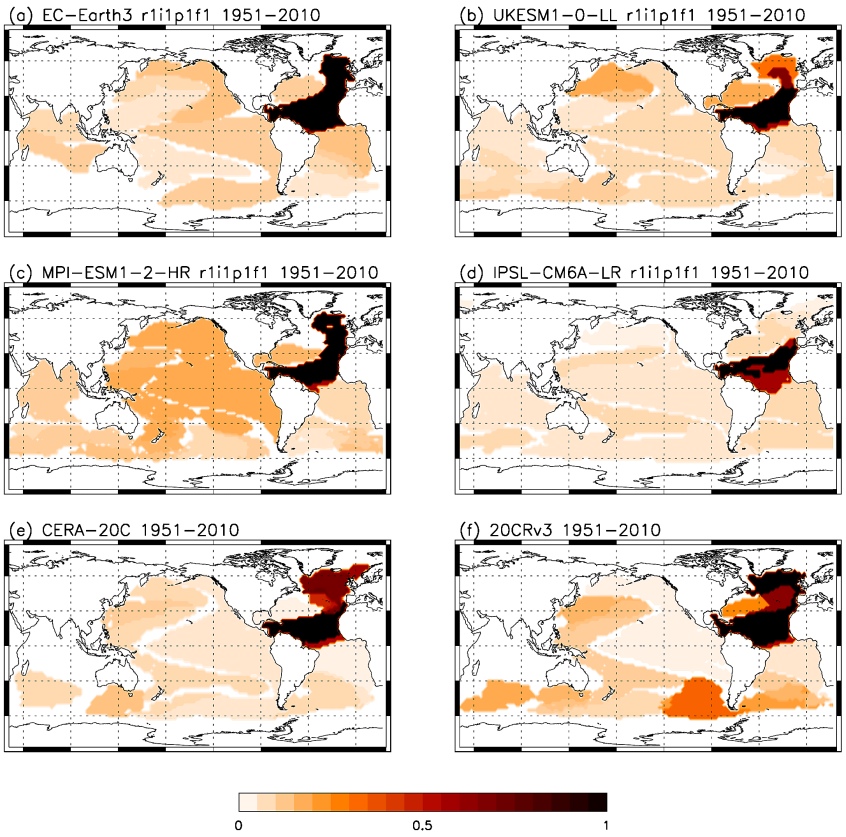


Figure S10: Spatially distributed maximum lagged distance correlation links between the AMO SST domain (black) and all other SST domains in reanalyses over the time period 1951–2010. (a) EC-Earth3, (b) UKESM1-0-LL, (c) MPI-ESM1-2-HR, (d) IPSL-CM6A-LR,(e) CERA-20C, (f) 20CRv3

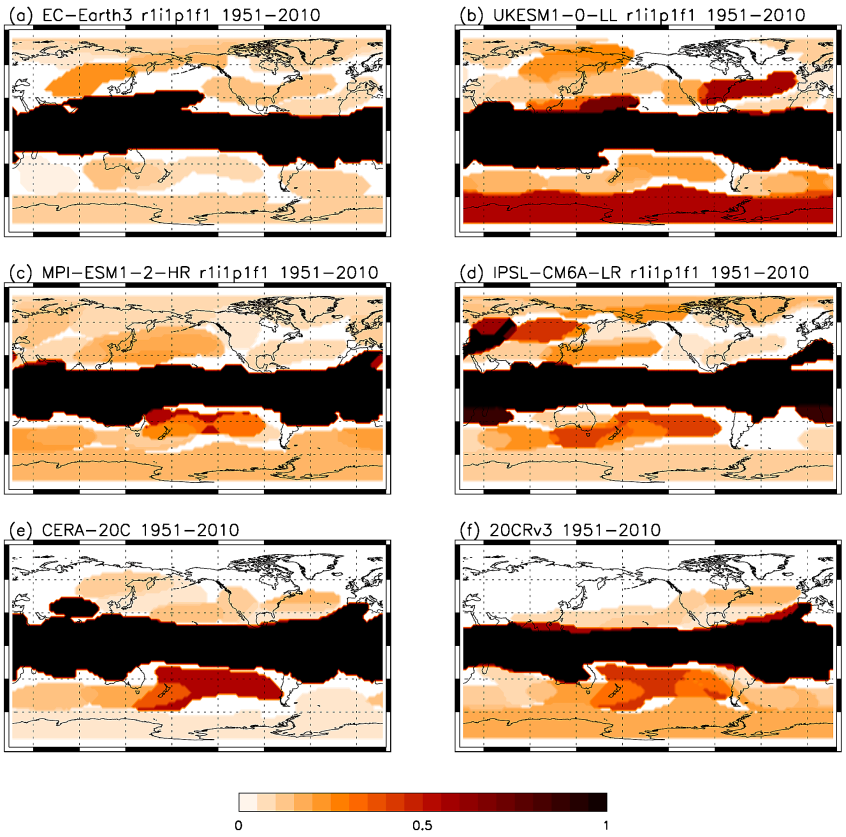


Figure S11: Spatially distributed maximum lagged distance correlation links between the TB Z500 domain (black) and all other Z500 domains in reanalyses over the time period 1951–2010. (a) EC-Earth3, (b) UKESM1-0-LL, (c) MPI-ESM1-2-HR, (d) IPSL-CM6A-LR,(e) CERA-20C, (f) 20CRv3

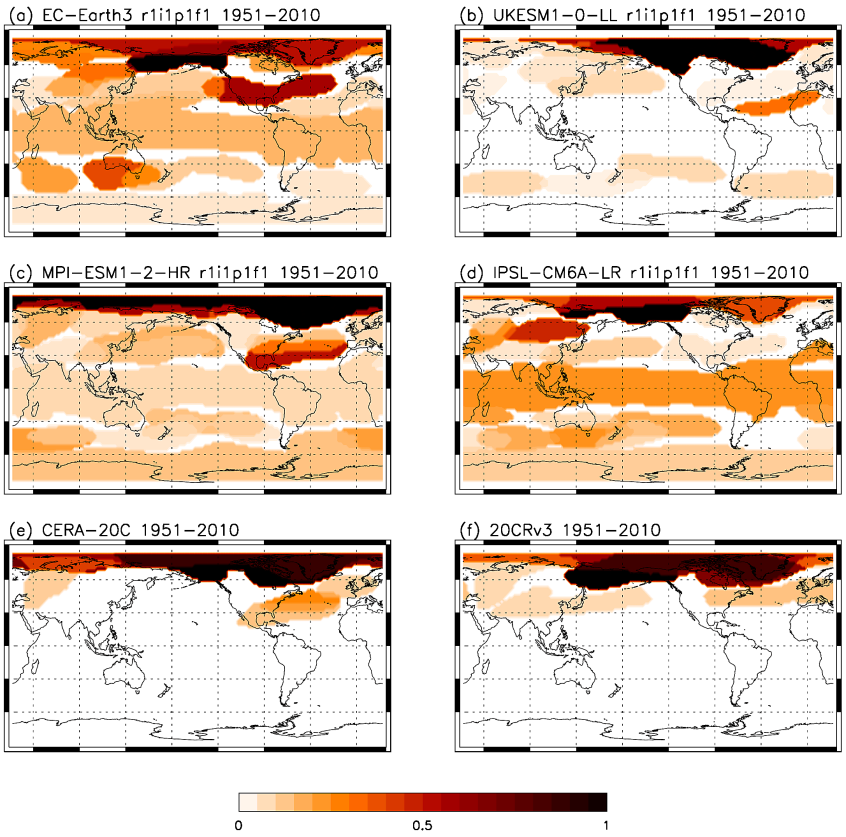


Figure S12: Spatially distributed maximum lagged distance correlation links between a North Polar Z500 domain (black) and all other Z500 domains in reanalyses over the time period 1951–2010. (a) EC-Earth3, (b) UKESM1-0-LL, (c) MPI-ESM1-2-HR, (d) IPSL-CM6A-LR,(e) CERA-20C, (f) 20CRv3

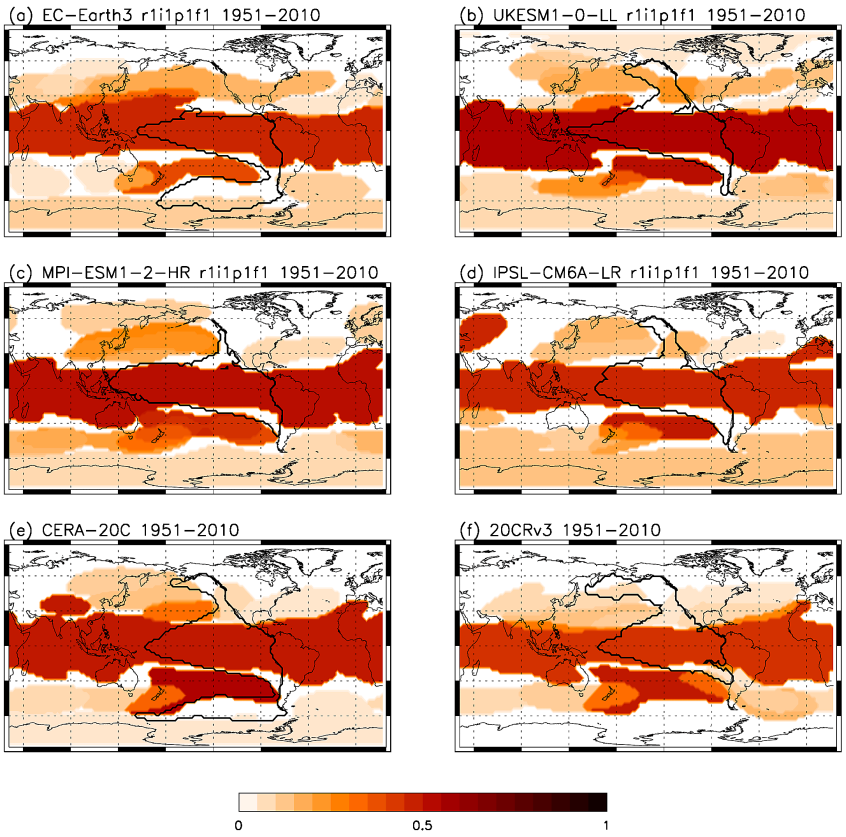


Figure S13: Spatially distributed maximum lagged distance correlation links between the ENSO SST domain (black) and all Z500 domains in reanalyses over the time period 1951–2010. (a) EC-Earth3, (b) UKESM1-0-LL, (c) MPI-ESM1-2-HR, (d) IPSL-CM6A-LR,(e) CERA-20C, (f) 20CRv3

Table S1: Interactions strength between domain triples in CERA-20C over 1901–2010

| SST | SST | Z500 | dMcor | $\sum$dCor |
|---|---|---|---|---|
| o3 | o7 | a15 | 0.188 | 1.080 |
| o3 | o10 | a15 | 0.200 | 1.140 |
| o3 | o11 | a15 | 0.193 | 1.156 |
| o7 | o11 | a10 | 0.174 | 1.108 |
| o7 | o10 | a12 | 0.242 | 1.552 |
| o7 | o11 | a12 | 0.283 | 1.655 |
| o7 | o8 | a15 | 0.183 | 0.935 |
| o7 | o10 | a15 | 0.281 | 1.529 |
| o7 | o11 | a15 | 0.300 | 1.601 |
| o8 | o10 | a15 | 0.165 | 0.899 |
| o8 | o11 | a15 | 0.186 | 1.037 |
| o9 | o11 | a15 | 0.146 | 1.023 |
| o10 | o11 | a10 | 0.184 | 1.028 |
| o10 | o11 | a12 | 0.313 | 1.627 |
| o10 | o11 | a15 | 0.327 | 1.585 |

| SST | SST | SST | dMcor | $\sum$dCor |
|---|---|---|---|---|
| o3 | o7 | o10 | 0.183 | 1.179 |
| o3 | o7 | o11 | 0.150 | 1.159 |
| o3 | o10 | o11 | 0.160 | 1.099 |
| o6 | o7 | o11 | 0.119 | 0.869 |
| o6 | o10 | o11 | 0.130 | 0.867 |
| o7 | o8 | o10 | 0.162 | 1.108 |
| o7 | o8 | o11 | 0.199 | 1.209 |
| o7 | o9 | o10 | 0.150 | 1.301 |
| o7 | o9 | o11 | 0.195 | 1.359 |
| o7 | o10 | o11 | 0.403 | 1.902 |
| o8 | o10 | o11 | 0.173 | 1.054 |
| o9 | o10 | o11 | 0.165 | 1.211 |
| o14 | o15 | o16 | 0.118 | 0.968 |

| SST | Z500 | Z500 | dMcor | $\sum$dCor |
|---|---|---|---|---|
| o7 | a12 | a15 | 0.188 | 1.349 |
| o8 | a9 | a10 | 0.236 | 1.268 |
| o10 | a12 | a15 | 0.246 | 1.442 |
| o11 | a10 | a15 | 0.191 | 1.081 |
| o11 | a12 | a15 | 0.274 | 1.580 |

Table S2: Similarity (NQS) of individual SST and Z500 domains between CERA-20C and 20CRv3 over 1901–2010

| SST domain in CERA-20C | most similar domain in 20CRv3 | NQS | SST domain in 20CRv3 | most similar domain in CERA-20C | NQS |
|---|---|---|---|---|---|
| o1 | o13 | 0.74 | o1 | o15 | 0.74 |
| o2 | o2 | 0.61 | o2 | o2 | 0.61 |
| o3 | o3 | 0.73 | o3 | o3 | 0.73 |
| o4 | o2 | 0.44 | o4 | o6 | 0.64 |
| o5 | o7 | 0.48 | o5 | o9 | 0.47 |
| o6 | o4 | 0.64 | 6 | o7 | 0.67 |
| o7 | o8 | 0.70 | o7 | o8 | 0.66 |
| o8 | o7 | 0.66 | o8 | o7 | 0.70 |
| o9 | o10 | 0.62 | o9 | o11 | 0.73 |
| o10 | o8 | 0.68 | o10 | o9 | 0.62 |
| o11 | o9 | 0.73 | o11 | o13 | 0.68 |
| o12 | o14 | 0.63 | o12 | o12 | 0.51 |
| o13 | o11 | 0.68 | o13 | o1 | 0.74 |
| o14 | o11 | 0.61 | o14 | o12 | 0.63 |
| o15 | o1 | 0.74 | | | |
| o16 | o1 | 0.56 | | | |

| Z500 domain in CERA-20C | most similar domain in 20CRv3 | NQS | Z500 domain in 20CRv3 | most similar domain in CERA-20C | NQS |
|---|---|---|---|---|---|
| a1 | a16 | 0.60 | a1 | a12 | 0.45 |
| a2 | a13 | 0.69 | a2 | a12 | 0.63 |
| a3 | a4 | 0.73 | a3 | a4 | 0.65 |
| a4 | a3 | 0.64 | a4 | a3 | 0.73 |
| a5 | a10 | 0.46 | a5 | a4 | 0.54 |
| a6 | a17 | 0.70 | a6 | a7 | 0.71 |
| a7 | a6 | 0.71 | a7 | a9 | 0.62 |
| a8 | a9 | 0.69 | a8 | a10 | 0.59 |
| a9 | a7 | 0.62 | a9 | a8 | 0.69 |
| a10 | a8 | 0.59 | a10 | a14 | 0.66 |
| a11 | a11 | 0.60 | a11 | a11 | 0.60 |
| a12 | a2 | 0.63 | a12 | a13 | 0.71 |
| a13 | a12 | 0.71 | a13 | a14 | 0.70 |
| a14 | a13 | 0.70 | a14 | a12 | 0.47 |
| a15 | a15 | 0.62 | a15 | a15 | 0.62 |
| | | | a16 | a1 | 0.60 |
| | | | a17 | a6 | 0.70 |